Poly(dimethylsiloxane)urethane-*co*-poly(methyl methacrylate) with 2,4-Toluene Diisocyanate and *m*-Xylene Diisocyanate. I. Compatibility and Impact Strength of Copolymers

CHEN-CHI M. MA,[1] YI-CHANG DU,[1] FENG-YIH WANG,[1] HUI-CHUNG WANG,[1] JEN-CHANG YANG[2]

[1] Department of Chemical Engineering, National Tsing-Hua University, Hsin-Chu 30043, Taiwan

[2] Chemicals System Research Division, Chung-Shan Institute of Science and Technology, Lung-Tan, Taiwan

Received 17 August 2000; accepted 31 January 2001

ABSTRACT: In this study, slightly crosslinked poly(dimethylsiloxane)urethane-*co*-poly-(methyl methacrylate) (PDMS urethane-*co*-PMMA) graft copolymers based on two diisocyanates, 2,4-toluene diisocyanate (2,4-TDI) and *m*-xylene diisocyanate (*m*-XDI), were successfully synthesized. Glass-transition behaviors of the copolymers were investigated. Results confirm that PDMS–urethane and PMMA are miscible in the 2,4-TDI system, but are only partially miscible in the *m*-XDI system. The methylene groups adjoining the isocyanate in the *m*-XDI system show increased phase-separation behavior over the 2,4-TDI system, in which the benzene ring adjoins the isocyanate. The functional group of PDMS–urethane improves the impact strength of the copolymers. The toughness depends on the compatibility of PDMS–urethane and PMMA segments in the copolymers. In the *m*-XDI system, the impact strength of the copolymer containing 3.75 phr macromonomer achieves a maximum value (from 13.02 to 22.21 J/m). The fracture behavior and impact strength of the copolymers in the 2,4-TDI system are similar to that of PMMA homopolymer, although they are independent of the macromonomer content in the copolymer. J Appl Polym Sci 83: 1875–1885, 2002

Key words: 2,4-TDI; *m*-XDI; PDMS-*g*-PMMA; compatibility; impact

INTRODUCTION

Poly(methyl methacrylate) (PMMA) prepared by free-radical polymerization exhibits high transparency, weather resistance, and nontoxicity. However, the low impact strength, lower thermal stability, and low abrasion resistance limit its applications.

Polydimethylsiloxane (PDMS) possesses many unique properties such as low T_g, good thermal stability, and low surface energy, which can improve the properties of PMMA by blending PDMS with PMMA physically or combining them through chemical techniques.[1–8] This study focuses on the PDMS-*graft*-PMMA. However, the solubility parameter of PDMS [15.34 $(J/cm^3)^{1/2}$] is different from that of PMMA [18.6 $(J/cm^3)^{1/2}$]. Thus, if PDMS-*g*-PMMA does not contain any other functional groups that can improve the com-

Correspondence to: C.-C. Ma (ccma@che.nthu.edu.tw).
Contract grant sponsor: National Science Council (Taiwan, Republic of China); contract grant number: NSC-88-2216-E007-016.

Journal of Applied Polymer Science, Vol. 83, 1875–1885 (2002)

DOI 10.1002/app.2315

patibility of PDMS and PMMA, the copolymer will show phase separation.[7]

Considering the intermolecular association, hydrogen bonding is a stronger intermolecular force than Van der Waals force, which can improve the compatibility of two structurally different polymers.[9,10] In this study, urethane groups are anticipated to be associated with the PDMS–oligomer chain ends and to improve the compatibility of PDMS–urethane and PMMA in the copolymer by hydrogen bonding between urethanes of PDMS–urethane and ester groups of PMMA. However, it was previously reported that the structural difference in the diisocyanates may affect the properties of urethane-containing polymers.[11]

In this study, 2,4-toluene diisocyanate (2,4-TDI) and *m*-xylene diisocyanate (*m*-XDI) were chosen to synthesize two types of urethane-containing PDMS-*co*-PMMA graft copolymers. Although several methods were suggested to react PDMS with PMMA into graft coploymers,[4–8] the macromonomer technique of synthesizing graft coploymers is more attractive because it has several advantages. For instance, the number and chain length of the graft branches can be easily controlled by the macromonomer method; thus, in this study, PDMS urethane-*co*-PMMA graft copolymers were prepared by the macromonomer technique. The compatibility and impact strength of PDMS urethane-*co*-PMMA graft copolymers resulting from the structural differences between 2,4-TDI and *m*-XDI are discussed.

EXPERIMENTAL

Materials

α,ω-Bis(hydroxypropyl) poly(dimethylsiloxane) (PDMS-diol) (tradename: X-22-160-AS) was obtained from Shin-Etsu Chemical Company, Japan. The molecular weight of PDMS-diol, 1037, was determined by quantitatively analyzing the hydroxyl groups of PDMS-diol. *m*-XDI, 2,4-TDI, and hydroquinone were purchased from Tokyo Chemical Industry Company, Japan. Methyl methacrylate (MMA), 2-hydroxyethyl methacrylate (HEMA), and anhydrous methanol were obtained from Aldrich Chemical Co. (Milwaukee, WI). Stannous octoate and azobisisobutyronitrile (AIBN) were obtained from Lancaster Synthesis Company and Showa Chemical Company, Japan, respectively. PDMS-diol was dried under vacuum at 60°C for 6 h. MMA and HEMA were purified by vacuum distillation. Other reactants and reagents were used as received.

Synthesis of Macromonomers

Two types of PDMS–urethane–methacrylate macromonomers based on 2,4-TDI and *m*-XDI were synthesized by adding 2*M* PDMS-diol with 0.15 wt % stannous octoate into benzene solution containing *m*-XDI or 2,4-TDI 10 wt % and stirring at 60°C in a dry atmosphere. When the absorption peak of hydroxyl groups in the IR spectra disappeared, equimolar amounts of methanol and HEMA containing 1 wt % hydroquinone were added into the mixture and the temperature was kept below 60°C to prevent thermal polymerization. When the absorption peak of the isocyanate group at 2270 cm^{-1} in the IR spectra became absent, the reaction was completed. The contaminants were removed from the reaction mixture by decolorizing carbon and the solvent was evaporated by vacuum distillation.

In this study, the macromonomer based on 2,4-TDI and hydroxyl-containing reactants is referred to as PRETDI; the macromonomer originating from *m*-XDI is represented by PREXDI.

Synthesis of PDMS Urethane-*co*-PMMA

Various amounts of PDMS–urethane macromonomers and MMA monomers were mixed and copolymerized by adding 0.3 wt % AIBN at 60°C in nitrogen atmosphere. Because the viscosity of the reaction mixture was raised rapidly, it was cooled down to room temperature and was then transferred to a mold that consisted of two sheets of glass. The copolymerization proceeded again at 60°C for 12 h and 90°C for 3 h. The reaction was completed when the absorption peak of carbon–carbon double at 1650 cm^{-1} in the IR spectra was absent. The pure PMMA specimen was synthesized by the same method without macromonomers.

In this study, the symbols SiTY and SiXY are used to represent the copolymers, where Si is the siloxane monomer, T is 2,4-TDI, X is *m*-XDI, and Y is the content of diisocyanate in phr units (i.e., part per hundred parts of copolymer), used to indicate the content of copolymer. For instance, SiT22.5 represents the copolymers based on 22.5 phr 2,4-TDI macromolecules.

Characterization

The PRETDI and PREXDI formed were characterized by IR, GPC, and NMR. The characteristic

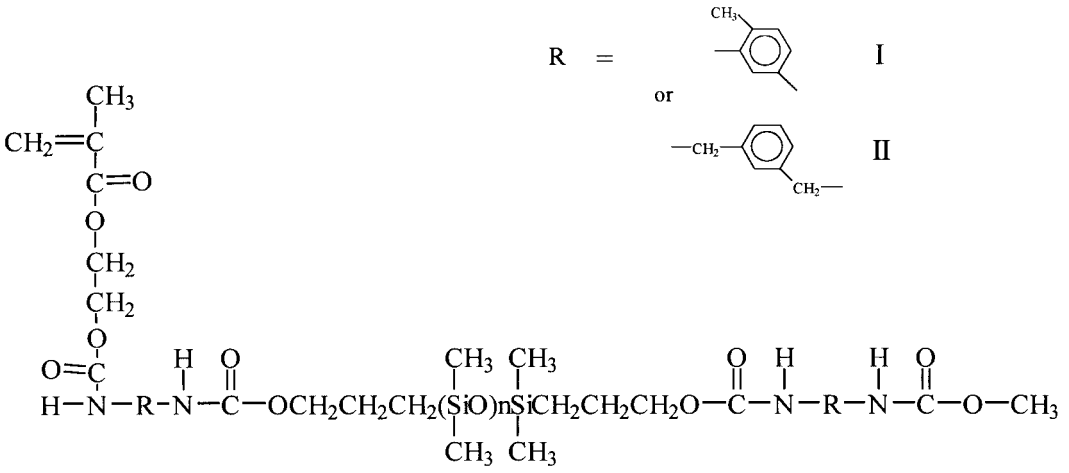

Figure 1 Structures of macromonomers.

absorption peaks of macromonomers in the IR and NMR spectra were detected by using a Perkin–Elmer IR-842 infrared spectrometer (Perkin Elmer Cetus Instruments, Norwalk, CT) and a Bruker AM 400-MHz ^{1}H–NMR spectrometer (Bruker Instruments, Billerica, MA), respectively. The chemical shift (δ) of the NMR spectra is given in ppm, and $CDCl_3$ was a solvent. The molecular distribution of macromonomers was measured by using a Waters 510 GPC (Waters Instruments, Rochester, MN), equipped with a refractive index detector, using tetrahydrofuran (THF) as the mobile phase at a flow rate of 1 mL/min at 40°C.

The damping factor (tan δ) of the polymer was measured as a function of temperature at 1 Hz, using a TA DMA 2980 dynamic mechanical analyzer (DMA; TA Instruments, New Castle, DE). A heating rate of 3°C/min was used. Samples were tested by using the dual-cantilever mode. The glass-transition temperatures of the copolymers were detected by using a TA DSC 10 differential scanning calorimeter (DSC) at a heating rate of 10°C in N_2 atmosphere.

The transparency of copolymer was measured from the transmittance of visible light through the specimen with a visible spectrometer.

Notched Izod impact strength was measured by an Izod type, TMI-43–1 Model Impact tester (Testing Machine Inc.), following the ASTM D256 method.

The morphological features on the fracture surfaces of fractured specimens were observed by a scanning electron microscope (SEM; JEOL, Japan).

RESULTS AND DISCUSSION

Characterization

Figure 1 shows the molecular formulae of macromonomers that were synthesized. The macromonomer containing 2,4-tolulene groups (I) is called PRETDI and the macromonomer containing *m*-xylene groups (II) is called PREXDI.

Figure 2 shows the IR spectra of PRETDI and PREXDI. No characteristic absorption peaks of isocyanate and hydroxyl groups can be observed. The absorption peak of urethane groups at 3400 cm^{-1} appeared in the IR spectra of PRETDI and PREXDI. The preceding observation shows that the isocyanate and hydroxyl groups were completely reacted and transformed into urethane groups. The ^{1}H–NMR spectra of PRETDI and PREXDI are shown in Figure 3(A) and (B), respectively. The protons of the vinyl group shift to both 5.58 and 6.13 ppm. The hydrogen in the urethane group of PREXDI shifts to 5.123 ppm, whereas the hydrogen of the urethane group of PRETDI possesses chemical shifts of 6.728 and 7.757 ppm.

Although the reactants are stoichiometric, the reactivity parameters and reaction conversion may limit the chemical homogeneity of macromonomers. Chemical heterogeneity leads to a few macromonomers that contain more or less one vinyl group in synthesized products. Copolymers, synthesized by copolymerizing such macromonomers with MMA monomers, are slightly crosslinked and contain a few macromonomers that have no reactivity. The swelling measurement was used to investigate the degree of crosslinking polymer. The soluble frac-

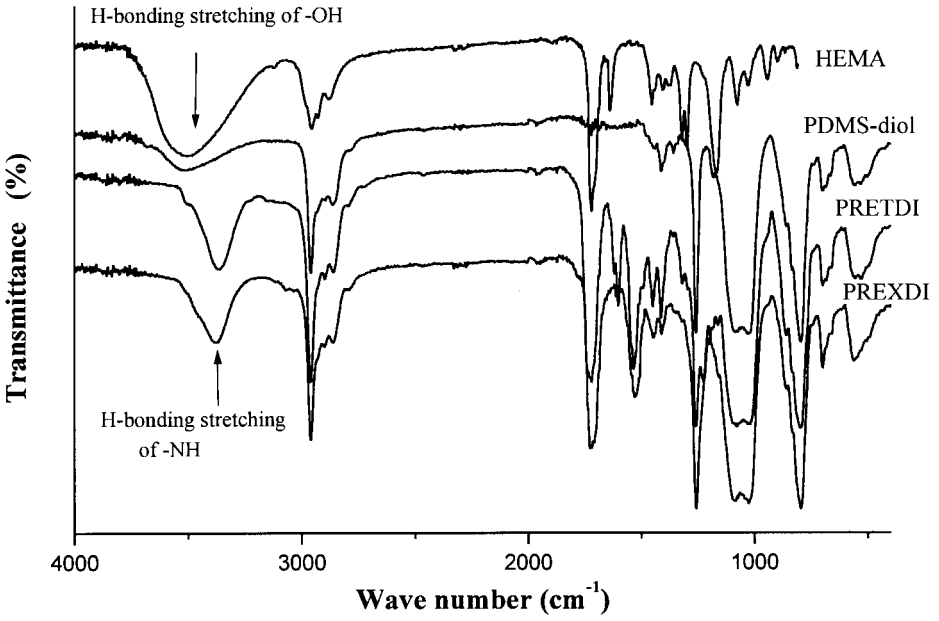

Figure 2 IR spectra of HEMA, PDMS-diol, PRETDI, and PREXDI.

tions of copolymer specimens, which include nonreactive macromonomers and nonnetwork polymers, were determined by Soxhlet extraction using THF as solvent at the boiling point of THF for 3 days. The crosslinking densities of copolymers were obtained by determining the difference in volume of the specimens before and after swelling the specimens with THF at room temperature for 1 week.[12]

The number-average molecular weights (M_n) of PREXDI and PRETDI were measured by NMR and are listed in Table I. A good correspondence between theoretical values and NMR results is obtained. The polydispersity indices (i.e., molecular weight distribution) of PREXDI and PRETDI are also presented in Table I. Table I also lists the content of the soluble fraction and crosslinking densities of copolymers in the two systems. The results indicate that those copolymers are slightly crosslinked and contain less than 2 wt % soluble species.

Compatibility of PDMS–Urethane and PMMA Segments of Copolymers in the *m*-XDI and 2,4-TDI Systems

The dynamic mechanical behavior of copolymer depends on the miscibility of a polymer pair. If the polymer pair is miscible, only one phase is formed and one sharp glass transition will be observed. Conversely, if two polymers are totally immiscible, two glass transitions will be observed, that is, at the glass transitions of the homopolymers.

Figure 4 shows the loss tangent (tan δ) spectra of PMMA homopolymer and copolymers in the 2,4-TDI and *m*-XDI systems detected by DMA. The tan δ peak is associated with the partial loosening of the polymer structure, so that the functional groups and the small chain segment can move.[13] The tan δ trace of PMMA in Figure 4 shows α-relaxation (i.e., the onset of long-range, coordinated molecular motion) at 137°C. In addition, β- and γ-relaxations (i.e., the rotation of the ester side group and the rotation of the α-methyl group, respectively) are also present at 50 and -100°C, respectively.

The tan δ curve of SiX22.5 in Figure 4 shows α-relaxations of PMMA and PDMS segments at 131 and -110°C, respectively. The α-relaxations of PMMA segments in SiX22.5 shift to a lower temperature compared with PMMA homopolymer. These results show that PDMS–urethane and PMMA segments in the *m*-XDI system are only partially miscible. Furthermore, a distinct peak is observed at -74°C in the tan δ curve of SiX22.5. A similar result is also present in PMMA-*g*-PDMS, as reported by Smith et al.[7] They proposed that the degree of mixing might be extended beyond the interface region between the PMMA and PDMS microdomains. The tan δ curve of SiT22.5 in Figure 4 confirms that PDMS–urethane and PMMA segments are well mixed. The α-relaxation of PMMA segments in SiT22.5 appears at 126°C, rather far from that of SiX22.5.

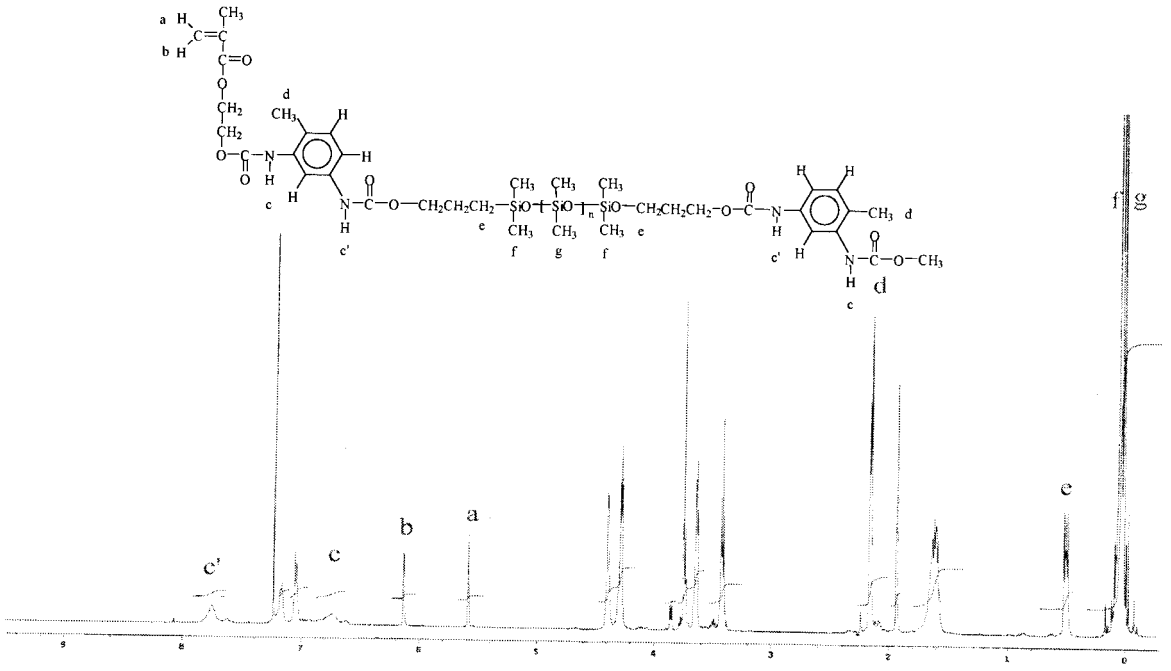

A

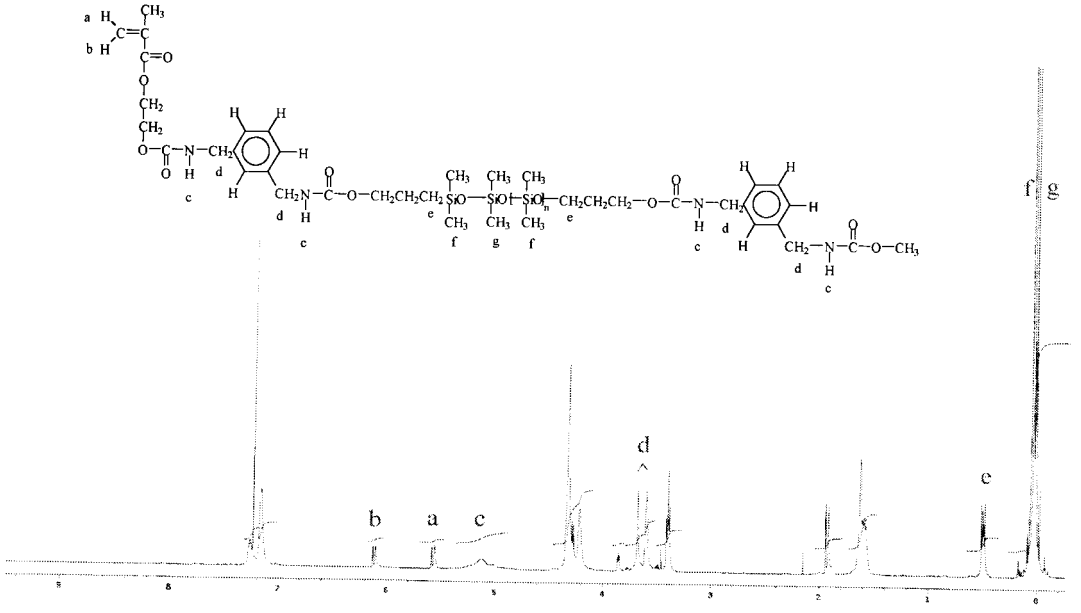

B

Figure 3 ^{1}H–NMR spectra of PRETDI (A) and PREXDI (B).

Table I Swelling Ratios of Copolymers and Molecular Weights of PRETDI and PREXDI

	PRETDI		PREXDI	
Test Method	GPC	NMR[a]	GPC	NMR[a]
M_n	1593	1602 (1547)	1776	1686.5 (1575)
M_w	1768	—	2300	—
Polydispersity index	1.4685	—	1.2951	—
	SiT3.75	SiT22.5	SiX3.75	SiX22.5
Swelling ratio	4.157	3.268	5.883	3.721
Soluble fraction (wt %)	1.74	1.21	1.89	1.42

[a] Theoretical values are in parentheses.

On the other hand, the α-relaxation of PDMS segments in SiT22.5 is less significant but a broad transition is observed at around -90°C. The result indicates that the compatibility of copolymer in the 2,4-TDI system is better than that in the *m*-XDI system.

The relationship between PDMS–urethane content and the glass-transition temperature (T_g) of PMMA segments in the two system copolymers was measured by DSC and is shown in Figure 5. Low-temperature transitions of PDMS are not distinct by DSC. Results measured by DSC correspond well with those measured by DMA. As seen in Figure 5, the T_g's of the copolymers in the *m*-XDI system are all the same and are independent of the macromonomer content, although T_g values are all lower than that of the PMMA homopolymer. On the other hand, in the 2,4-TDI system, the T_g's of PMMA segments of the copolymers decrease with increasing macromonomer content, indicating that the system is miscible.

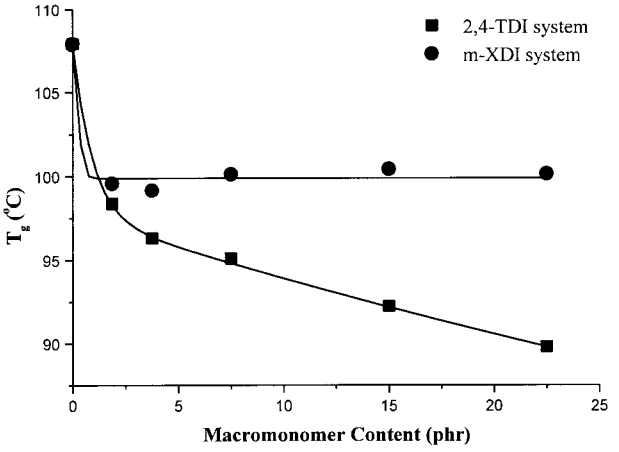

Figure 5 Relationship between T_g and macromonomer content in the copolymers.

In addition to the glass-transition behavior, the compatibility of a polymer pair can be determined by observing the optical clarity of the copolymer. The amount of light scattered depends on the size of the domains. Thus, if a polymer pair is immiscible (i.e., appearance of phase separation) and forms reasonably large domains (larger than 20 nm), the copolymer will be hazy, cloudy, or milky white to the eye.[14] Figure 6 shows the

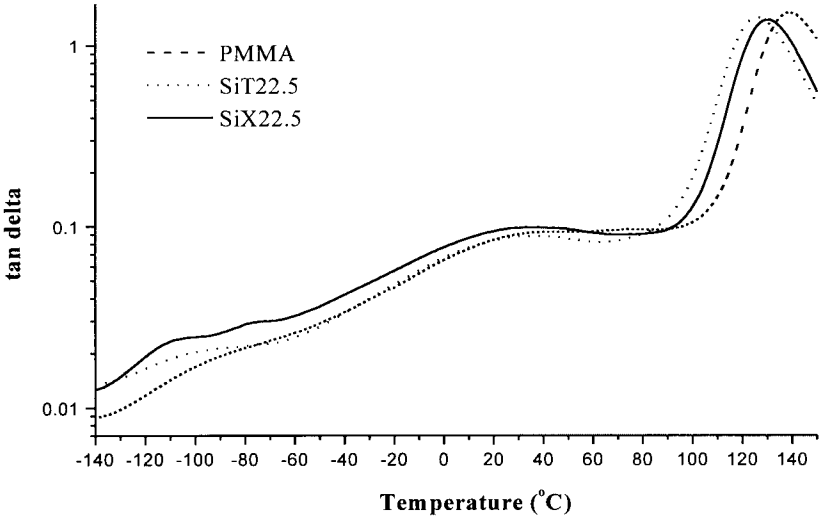

Figure 4 Tan δ traces of PMMA, SiX22.5, and SiT22.5.

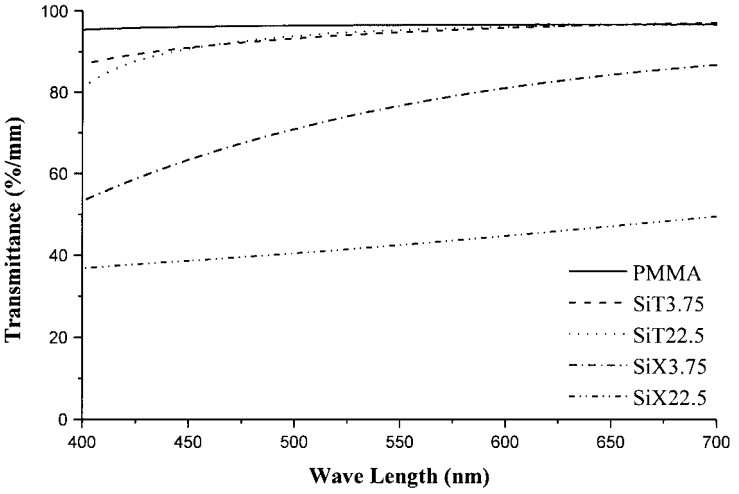

Figure 6 Visible spectra of PMMA and various contents of 2,4-TDI copolymers.

visible spectra of PMMA and copolymers in the 2,4-TDI and *m*-XDI systems. The scale of the spectrum is given as the transmittance per thickness of specimens. PMMA homopolymer exhibits optical transparency and high transmittance in all regions of the visible spectrum in Figure 6. Results of copolymers in the 2,4-TDI system are similar to those of the PMMA hompolymer, again showing that PDMS–urethane and PMMA segments are miscible in the 2,4-TDI system. However, increasing the macromonomer content will decrease the transmittance of the visible spectrum and the appearance of such specimens is cloudy and milky-white in the *m*-XDI system. Results of the visible spectra in Figure 6 confirm that the PDMS–urethane and PMMA segments in the *m*-XDI system are immiscible.

From the preceding observations, the structural difference in the diisocyanates does affect the compatibility of PDMS–urethane and PMMA segments in the copolymer. Considering the structure of the copolymer, although both *m*-XDI and 2,4-TDI possess a *meta*-substituted aromatic group, the functional group that adjoins the isocyanate group dominates the resultant compatibility of urethane-containing polymers. The methylene groups adjoining the isocyanate in the *m*-XDI system result in increased phase-separation behavior over that of the 2,4-TDI system, in which only the benzene ring adjoins the isocyanate. In a subsequent report,[15] the reason for this difference in the compatibility between the 2,4-TDI and the *m*-XDI systems will be further investigated.

Impact Strength and Fracture Morphology of Copolymers in the 2,4-TDI and *m*-XDI Systems

Figure 7 shows the notched Izod impact strength of copolymers in the 2,4-TDI and *m*-XDI systems versus the macromonomer content in copolymers. In the 2,4-TDI system, the impact-resistance behavior of the copolymers is similar to that of PMMA homopolymer, and is independent of the macromonomer content in the copolymer. However, the impact strength of the copolymer in the *m*-XDI system increases from 0.24 to 0.416 ft-lb/in. (the maximum value), as the macromonomer content in the copolymer increases to 3.75 phr; thereafter, the impact strength of copolymer decreased with increasing macromonomer content.

The difference in the impact-resistance behavior between the 2,4-TDI and *m*-XDI systems can be interpreted by examining the morphological features of fracture surfaces. Figure 8 is the SEM fractograph of the fracture surface of PMMA homopolymer next to the notched portion of the specimen. The fracture texture is smooth, and the crack initiates locally at several sites at the notched portion. Figure 9 shows a series of bands close to the notched portion of a fractured PMMA specimen, which is referred to as a "mackerel" structure and is caused by the biplanar fracture of craze fibrils.[16] Doyle[17] explained the formation mechanism of the mackerel structure on the fracture surfaces of PMMA. It was proposed that beyond some critical crack velocities, the craze preceding the crack front splits into several parallel fronts.[16,17] The crack branching absorbs enough energy to decelerate the crack velocity below the

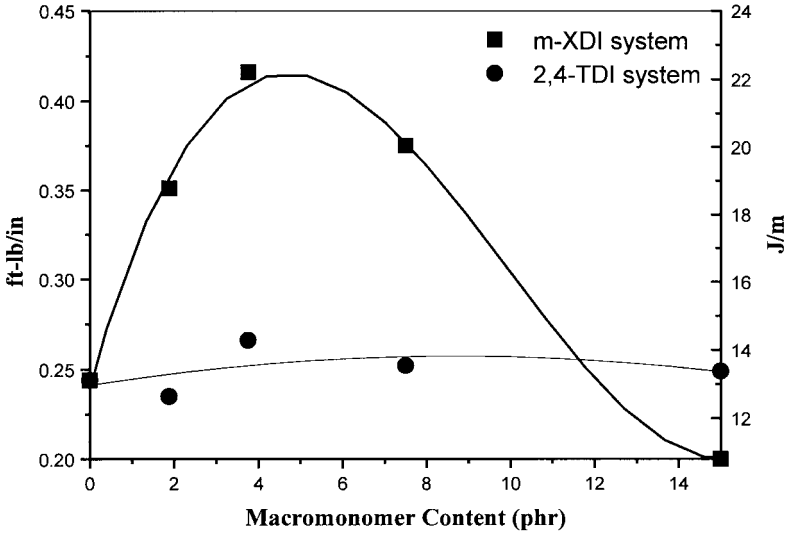

Figure 7 Notched Izod impact strength of poly(dimethylsiloxane)urethane-*co*-PMMA copolymers in the 2,4-TDI and *m*-XDI systems.

critical point. At this stage, the branching crazes would not be extended and the cracks are recombined into a single front. This fracture process is cyclic, and then a banded texture will be formed.

Figure 10 shows the morphological feature of crack initiation at SiX7.5 and also shows clear differences compared with PMMA homopolymer. The fracture surface next to the notched portion of the SiX7.5 specimen is shown in Figure 11. Instead of a smooth surface, the crack is composed of several fronts initiated on different planes along the notched portion. It shows that a large number of holes are spread on the rough surface. In addition, the copolymer matrix exhibits plastic deformation around these holes. The surface near the notch sites of SiX7.5 in Figure 11 also exhibits the rough texture at a higher magnification than that in Figure 12. The PDMS–urethane and PMMA segments in the *m*-XDI system are immiscible and the microdomains composed of PDMS–urethane spread throughout the bulk of the copolymer. Thus the holes should be the result of drawing up the microdomains during the fracture process.

From the preceding observations, it is apparent that the role of the rubbery microdomains is to initiate multiple craze growth in the copolymer matrix. Bucknall and coworkers[18,19] explain the

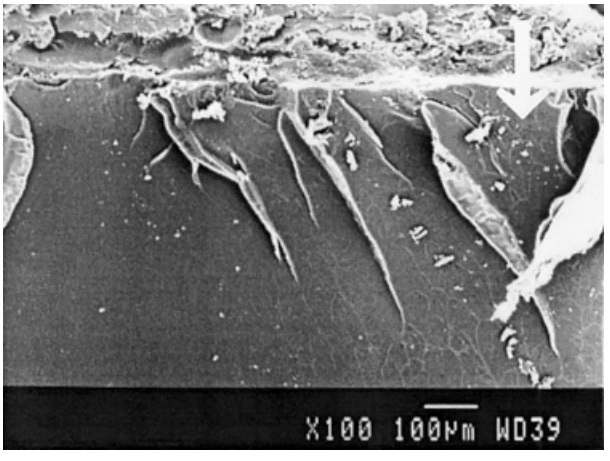

Figure 8 Fracture surface near the notch of PMMA. The arrow shows the propagation direction of crack.

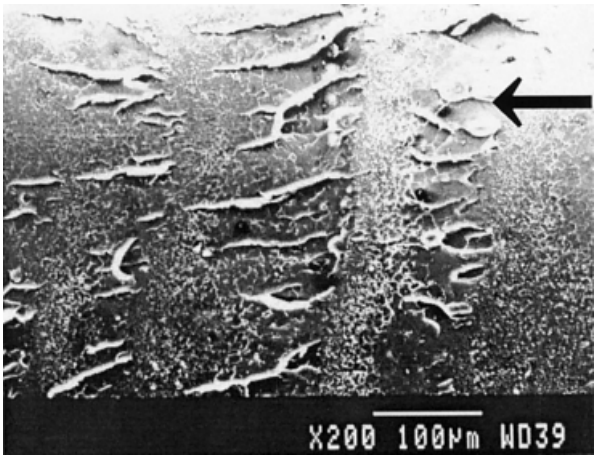

Figure 9 Fracture surface of PMMA. The arrow shows the propagation direction of crack.

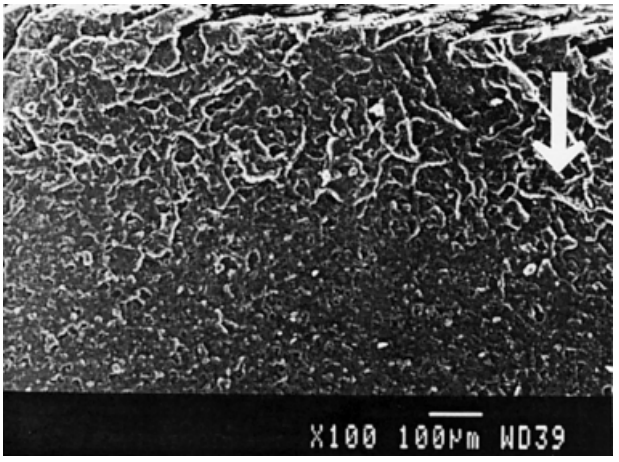

Figure 10 Fracture surface near the notch of SiX7.5. The arrow shows the propagation direction of crack.

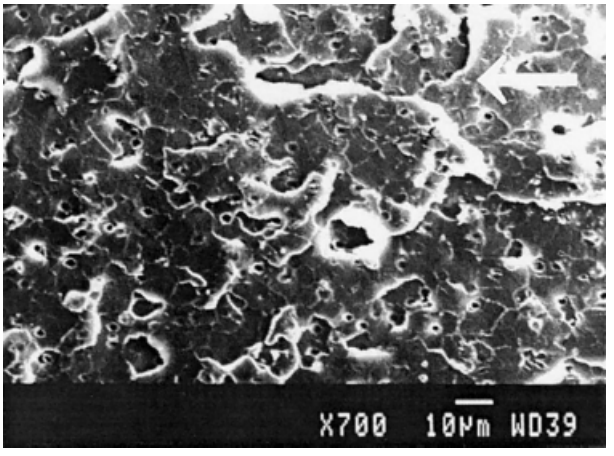

Figure 12 Fracture surface of SiX7.5 (magnification ×700). The arrow shows the propagation direction of crack.

formation and function of multiple crazing initiated from the rubber particles (or referred to as microdomains in this study) throughout the brittle polymer matrix. They proposed that, under an applied tensile stress, crazes would be initiated at the points of maximum stress concentrations, which are usually around the rubber particles in the matrix. As a result, a large number of small crazes are formed, in contrast with the small number of large crazes formed in the same polymer in the absence of rubber particles. The multiple crazing that occurs throughout a comparatively large volume of rubber-modified material is accompanied by the high-energy absorption in the fracture process.

The fracture texture next to the notched sites of SiX15, as seen in Figure 13, becomes smooth. Figure 14 shows that the cracks initiated near the notched sites of specimens tend to recombine with each other to generate a small number of large cracks. In terms of the energy absorption, such fracture behavior is accompanied by low impact resistance. The observation of the fracture behavior of SiX15 corresponds to the result that the impact resistance decays and is even less than that of pure PMMA.

Figures 15 and 16 show the features that are near to and far from the notched sites of SiT15, respectively. Because the copolymer contains a substantial amount of PDMS–urethane, the crack initiates locally at a few sites at the notched

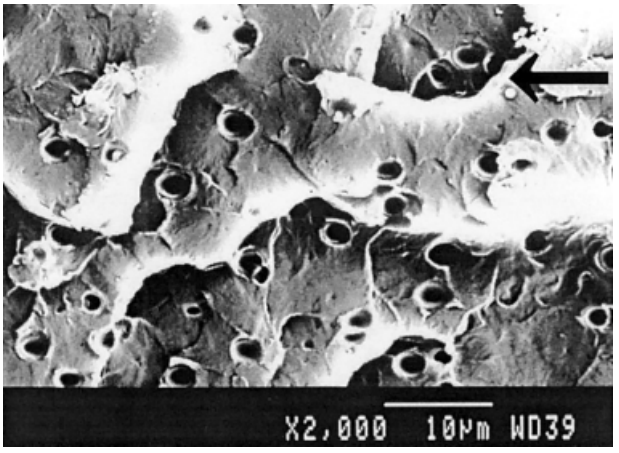

Figure 11 Fracture surface of SiX7.5 (magnification ×2000). The arrow shows the propagation direction of crack.

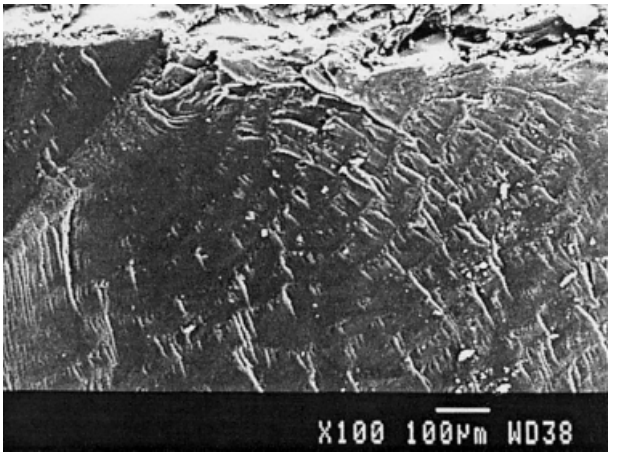

Figure 13 Fracture surface near the notch of SiX15. Crack initiated from the upper right-hand corner.

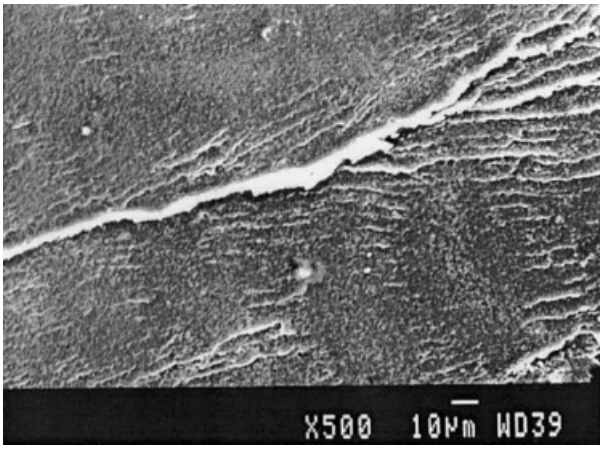

Figure 14 Fracture surface of SiX15. Cracks propagate from the upper right-hand corner to the bottom left-hand corner.

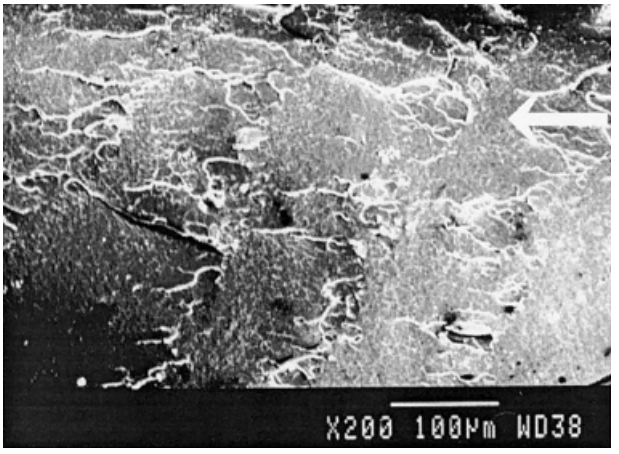

Figure 16 Fracture surface far away from the notch of SiT15. The arrow shows the propagation direction of crack.

portion, and the surface along the notch is smooth. Furthermore, the patterns of the fracture surface near the notched portion of SiT15 also show a "mackerel" structure. According to the fracture morphology and the results obtained by the impact measurement, the fracture behaviors of the copolymers in the 2,4-TDI system are similar to that of PMMA homopolymer, and are independent of the amount of macromonomer in the copolymer.

CONCLUSIONS

Slightly crosslinked PMMA-*co*-PDMS urethane graft copolymers based on MMA monomers and PDMS–urethane–methacrylate macromonomers with two diisocyanates, 2,4-toluene diisocyanate (2,4-TDI) and *m*-xylene diisocyanate (*m*-XDI), were successfully synthesized.

The glass-transition behaviors of copolymers in the two systems were measured by DMA and DSC. Results show that the structural differences in the diisocyanates affect the compatibility of PDMS–urethane and PMMA segments. Methylene groups adjoining the isocyanate in the *m*-XDI system show increased phase-separation behavior over that of the 2,4-TDI system, in which only the benzene ring adjoins the isocyanate. Therefore, PDMS–urethane and PMMA segments are miscible with PMMA in the 2,4-TDI system but are only partially miscible in the *m*-XDI system. The structures of the copolymers were confirmed by IR, NMR, GPC, Soxhlet extraction, and swelling measurement.

The function of the toughening matrix of PDMS–urethane in copolymer is dependent on the compatibility of PDMS–urethane and PMMA segments. In the *m*-XDI system, the impact strength of the copolymer containing 3.75 phr macromonomer reaches a maximum value (from 13.02 to 22.21 J/m). Conversely, PDMS–urethane and PMMA segments in the 2,4-TDI system are miscible. The fracture behaviors and strength of the copolymers in the 2,4-TDI system are similar to those of PMMA homopolymer, but are independent of macromonomer content in the copolymers.

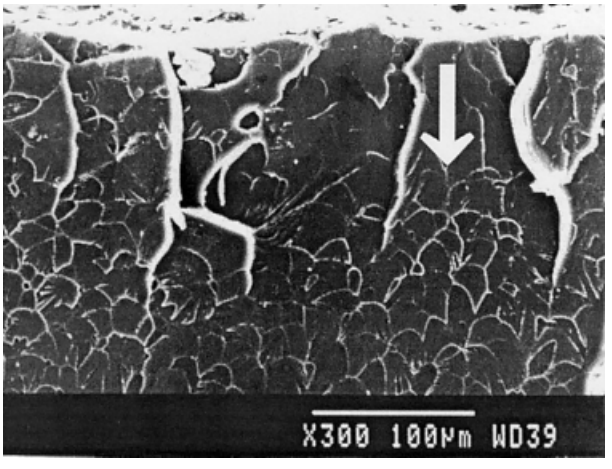

Figure 15 Fracture surface near the notch of SiT15. The arrow shows the propagation direction of crack.

This research was financially supported by the National Science Council, Taiwan, Republic of China, under Contract No. NSC-88-2216-E007-016.

REFERENCES

1. Sperling, L. H.; Sarge, H. D., III. J Appl Polym Sci 1972, 16, 3041.
2. Inoue, H.; Ueda, A.; Nagai, S. J Polym Sci Part A Polym Chem 1988, 26, 1077.
3. Blahovici, T. F.; Brown, G. R. Polym Eng Sci 1987, 27, 1611.
4. Chujo, Y.; Murai, K.; Yamashita, Y. Makromol Chem 1985, 186, 1203.
5. Kawakami, Y.; Karasawa, H.; et al. Polym J 1985, 17, 1159.
6. Kawakami, Y.; Murthy, R. A. N.; Yamashita, Y. Makromol Chem 1984, 185, 9.
7. Smith, S. D.; DeSimone, J. M.; Huang, H.; York, G.; Dwight, D. W.; Wilkes, G. L.; McGrath, J. E. Macromolecules 1992, 25, 2575.
8. Harvey, T. B., III; Scottsdale, A. U.S. Pat. 4,711,943, 1987.
9. Fowkes, F. M.; Tischler, D. O.; et al. J Polym Sci Polym Chem Ed 1984, 22, 547.
10. Kwei, T. K.; Pearce, E. M.; Ren, F.; Chen, J. P. J Polym Sci Part B Polym Phys 1986, 24, 1597.
11. Hepburn, C. Polyurethane Elastomers, 2nd ed.; Elsevier: London, 1992; Chapter 3.
12. Coleman, M. M.; Lee, K. H.; Skovanek, D. J.; Painter, P. C. Macromolecules 1988, 21, 59.
13. McGrum, N. G.; Hu, Q.; Gibson, H. W. Anelastic and Dielectric Effects in Polymer Solid; Dover: New York, 1967; Chapter 8.
14. Sperling, L. H. Polymeric Multicomponent Materials; Wiley: New York, 1997; Chapter 2.
15. Wang, F. Y.; Du, Y. C.; Ma, C.-C. M. J Polym Sci Part B Polym Phys to appear.
16. Hull, D.; Owen, T. W. J Polym Sci Polym Phys Ed 1973, 2039.
17. Dolyle, M. J. J Mater Sci 1983, 18, 687.
18. Bucknall, C. B. Rubber Chem Technol 1987, 60, 35.
19. Kinloch, A. J.; Young, R. J. Fracture Behaviour of Polymers; Elsevier: London, 1983; Chapter 11.